

Obstacle Avoidance Strategy of Mobile Robot Based on Wireless Sensor Networks

<https://doi.org/10.3991/ijoe.v12i11.6230>

An Peng
Ningbo University of Technology, Zhejiang, China

Abstract—In order to improve the real time performance, accuracy and stability, an obstacle avoidance strategy of mobile robot based on wireless sensor networks is proposed in this paper. The algorithm is combined with fuzzy control and neural network control theory which can express those rules difficult to describe by using mathematical model. Simulation results show that the obstacle avoidance strategy can improve the overall system performance substantially and is suitable for mobile robot intelligent control.

Index Terms—obstacle avoidance strategy, mobile robot, wireless sensor networks

I. INTRODUCTION

Nowadays, new technology is constantly emerging (cloud computing, big data, wireless sensors, etc.)[1-3], one of present focus research fields is mobile robot which is the important direction of robot research. The traditional mobile robots basically use the special processor and special operating system which cannot satisfy the modern robot's development request, with the development of embedded system, the robot with economization, miniaturization and intellectualization is developed. Obstacle avoidance is the important safeguard of safe travel for mobile robot, as well as one of the most important subjects for research. With the gradual development of the intelligent robot technology and the gradual spread of application field, research and development of intelligent home robot, being the center of interest in the rising research presently, has been becoming a high technology industry with promising future.

The robot obstacle avoidance and path planning is not only one of important research directions of mobile robots, but also an indispensable and important part of the mobile robots' navigation technology. The robot obstacle avoidance and path planning in static scenes is the core content of the global path planning as well as the basis of the local path planning. Multiple mobile robots system provides an unchallenged incentive to all researchers in the past two decades, with its distribution characters in time and space, as well as its high efficiency. Great interests have been attracted to application domains including industry, military, national defense, daily life, and deep space, etc. In the research of specific application tasks, such as transporting heavy object, arresting target and multi-sensors cooperative map exploration, etc., robots are required to form and maintain specific shapes of formation during the tasks' execution. And these lead to a rush in the research of multi-robot formation control, which is one of the key techniques in multi-robot cooperation and coordination.

The mobile robot has been used in many fields, such as military, industry, agriculture and service industry more and more widely with the continuous development of

society, as the basic of safe operation and high efficiency for robot in various environments, obstacle avoidance planning in recent years has become the focus of research in the field of robot. The key of obstacle avoidance planning is to formulate feasible strategy, so that, according to a certain standard, the robot can move from the start point to the target point without collision, so, a method is needed to solve the mobile robot obstacle avoidance planning problem based on the combination of clone selection algorithm and visual graph, in the course of the study, set the length of path as the standard of obstacle avoidance planning results, hunt for optimal path in a structured environment, then control the entity robot base on the optimal path. The purpose for obstacle avoidance strategy is to find out the optimal path between the start point and the target point, according to which, the entity mobile robot can move without collision, finally, realize the development of mobile robot system.

As the mobile robot path planning problem is nonlinear, multi standard and difficult to obtain the global optimum path, so there is some difficulty to solve this problem using traditional method. While the clone selection of artificial immune system algorithm can take various factors into consideration, and find optimal solutions through continuous optimization of the population, at the same time, clone selection has the characteristics of diversity, robustness and distribution, so, the algorithm can fully meet the needs of the obstacle avoiding planning problem for mobile robot. But the traditional clone selection algorithm has remarkable shortcoming: slow speed of convergence. In order to solve this problem, the traditional clone selection algorithm should be improved then, combine it with the visibility graph method, the improved algorithm can find for the optimal path and significantly improve the efficiency. It should be realized roaming behavior and target tracking behavior of mobile robot, then, apply the obstacle avoidance planning method for mobile robot based on clone selection and visibility graph in different environment, prove that the algorithm can meet requirements of robot obstacle avoidance planning, finally, control entity robot according to optimal path, prove that this algorithm can satisfy the needs of entity robot in the real environment.

II. OVERVIEW

The embedded mobile robot platform is designed and developed independently in Wei's paper [4], which is based on embedded system, it provides a solution of hardware and software design for mobile robot. The robot platform has the characteristic of Porting and expansibility, and the system of obstacle avoidance is studied in this platform. ARM microprocessor S3C2410 with high advanced capacity is used as the chief chip to design the bottom movement control system. Peripheral circuit and

expansion interface are designed; the module of step motor driven is emphatically designed. Based on the robot hardware design, the Porting of Linux operation system is achieved and the driver of step motor is developed. The ultrasonic sensor is used for environment survey of mobile robot and the distance measuring module of multi-sensor which is based on AT89C52 controller is designed, the precision of distance measuring can satisfy the request of obstacle avoidance by carrying on a series of experiments.

Neural fuzzy control algorithm is proposed in Pereira's paper [5], the design and implement of the algorithm is discussed in detail. The accuracy and the validity of the proposed algorithm is proved by the simulation results, the safe obstacle avoidance of mobile robot is realized by transplanting the algorithm into embedded mobile robot system. In the actual test, the design of the mobile robot's platform and the algorithm of obstacle avoidance can rapidly and efficiently achieve obstacle avoidance of the robot.

Stepper motor movement control system based on S3C44BOX+ μ C Linux system and advantage of stepper motor are introduced in Zhang's paper [6], including the design of stepper motor driver circuitry and development of device driver program in Embedded Linux system. Finally, the realization of software and hardware of ultrasonic measuring system and running process of automatic obstacle avoidance system are discussed, including design of ultrasonic measuring system circuitry and development of ultrasonic device driver program. According to obstacle avoidance algorithms, depended on periphery circumstance information from ultrasonic sensors, the application program designed in Linux running environment, is able to make use of stepper motor device driver and realize the function of obstacle avoidance and navigation.

Zhang's paper [7] researches on several technologies of autonomous obstacle avoidance which are used commonly at current stage, just as APF, ANNs and Fuzzy control. Then it design a set of Manipulator Mobile robot comprised by the PLC, motor drive, servomotor, communication module, main equipment and navigation modules etc., and based on which is to research autonomous obstacle avoidance of mobile robots. The ultrasonic sensor works simply and fast, so it is useful to accomplishing the real time controlling. Based on those, Wang's paper [8] takes it to detect the environment, and designs an autonomous obstacle avoidance control system which combined fuzzy algorithm with behavioral control. In Zou's paper [9] the robot obstacle avoidance behavior was divided into three acts: Heading the same behavior, avoidance behavior and conduct emergency stop. Ultimately, by completing a chain of physical experiments of the autonomous obstacle avoidance, the purpose of autonomous obstacle avoidance of the mobile robot and keep the same navigation after avoiding the obstacles was achieved. According to the results of physical experiments, the feasibility of the designed control system can be verified.

The structural features of 8D-WMM show the characteristics of redundancy, so the problems of its motion planning are more complicated than mobile robot and traditional redundant robot. Furthermore, because 8D-WMM generally works in complicated environments with obstacles, it is meaningful to enhance its operating ability by use of the redundancy in non-structural environment full of obstacles. Nowadays, it is lack of systematic study in framework integration of WMM and inverse kinematics

optimization facing obstacle avoidance throughout this field, which cannot fully exert the flexible operating ability of this kind of robot in complicated environment. Tao's paper [10] focuses on theoretical exploration on motion planning method of 8D-WMM including kinematics, path planning, obstacle avoidance, and end effector operation. Besides, the 8D-WMM system was built for elderly and disabled aid, and experiments were carried out to testify theories. Because the 8D-WMM includes constraint, it is difficult to obtain analytical solution of self-motion manifold. Therefore, based on the theory of movement equivalence, it is carried through study on its kinematics and solved 8D-WMM self-motion manifold by combining geometric distribution characteristics of 8D-WMM joint axes and using the tool such as vector algebra. And it also got Jacobian matrix by using the speed superposition principle through regarding mobile platform as Generalized Kinematic Pair.

To easily evaluate the obstacle avoidance capabilities of a redundant robot, Ling's paper [11] proposed and established obstacle avoidance ability index of redundant robot which has intuitive geometric meaning in virtue of space measurement of pole self-motion trajectory-obstacle avoidance activity, whose solution is obtained through a planar 3-DOF robot, and further analyzes the influence of 8D-WMM framework size on its obstacle avoidance ability by using the index. In the aspect of path planning study, the typical operating environment and obstacle of 8D-WMM were analyzed. Then the avoidable criterion of various obstacles such as flat top, slant, and dome, etc., was given by using the results of 8D-WMM self-motion analysis and combining the characteristics of arms joint configuration and the solution to the mobile manipulator's obstacle avoidance area was analyzed. The path planning algorithm of the mobile platform facing obstacle avoidance area and manipulator facing the outline of obstacles were presented. Through the trajectory tracking of a planar 3-DOF robot and the simulation examples of 8D-WMM implementation window, the algorithm feasibility is validated.

The key of obstacle avoidance planning is to formulate feasible strategy, so that, according to a certain standard, the robot can move from the start point to the target point without collision, so, a method is needed to solve the mobile robot obstacle avoidance planning problem based on the combination of clone selection algorithm and visual graph, in the course of the study, set the length of path as the standard of obstacle avoidance planning results, hunt for optimal path in a structured environment, then control the entity robot base on the optimal path.

III. METHOD AND ALGORITHM

The Obstacle Avoidance Control (OAC) is an experimental system, which is generated by using VR technology and is suitable for virtual experiments, including corresponding laboratory environment, related experimental instrument and equipment, experimental objects and experimental information resources. Students can observe one experiment object from different views in a simulated 3D experimental scenario on a computer in the OAC and can select or drag via the mouse to complete interaction with the virtual experimental objects. The virtual teaching laboratory system is designed and studied in order to provide a virtual experimental environment to users under which users can get different components, and connect

copy, move and delete them. The structure of a OAC platform is shown as the Fig. (1).

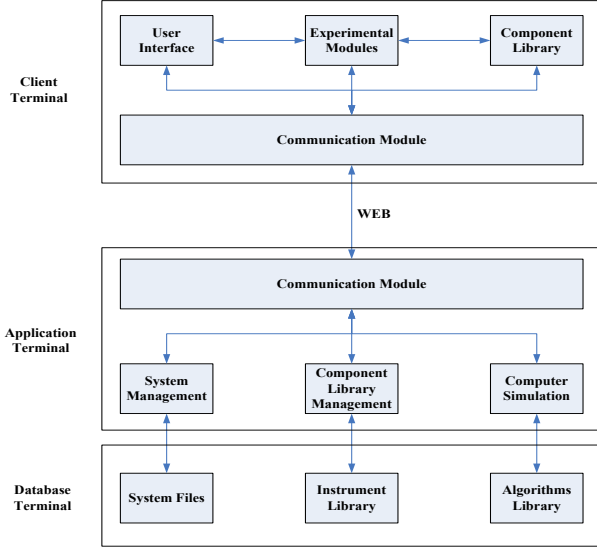


Figure 1. The basic structure of the platform

When the spatial relationship between the two adjacent connecting rods $i-1$ and i changes in accordance with the following motions, the coordinate transformation can be accomplished.

- 1) Revolve θ_i around axes Z_{i-1} until it reaches the position where axes Z_{i-1} is parallel to axes Z_i ;
- 2) Translate distance d_i along axes Z_{i-1} to cause X_{i-1} to be collinear with X_i
- 3) Translate distance λ_i along X_i to cause the coordinate system origins of the connecting rods to be coincided;
- 4) Revolve angle λ_i along X_i to cause axes Z_{i-1} to be collinear with axes Z_i

The basic algorithm is shown as the equation (1):

$$C^1 = C - C^0, e^1 = e - e^0, \eta^1 = \eta - \eta^0, \rho_1 = \rho - \rho_0 \quad (1)$$

$$f(x, \omega) = f^0(x, \omega) + \int_V S(x - x')(L^1 F(y') + \rho_1 \omega^2 \mathbf{g}(R) T_1 f(y')) S(y') dy' \quad (2)$$

The we get:

$$\begin{aligned} & \frac{1}{\Gamma(1+\alpha)} \int_R \frac{f(t)}{(t-x)^\alpha} (dt)^\alpha \\ & = \lim_{\varepsilon \rightarrow 0} \left[\frac{1}{\Gamma(1+\alpha)} \int_{-\infty}^{x-\varepsilon} \frac{f(t)}{(t-x)^\alpha} (dt)^\alpha + \frac{1}{\Gamma(1+\alpha)} \int_{x+\varepsilon}^{\infty} \frac{f(t)}{(t-x)^\alpha} (dt)^\alpha \right] \\ & g_{ik}(\bar{k}, \omega) = -\frac{1}{\eta_{11}^0} \frac{1}{\bar{k}^2} + \frac{1}{\rho_0 \omega^2} \left(\frac{e_{15}^0}{\eta_{11}^0} \right)^2 \frac{\beta_\perp^2}{\bar{k}^2 - \beta_\perp^2}, \\ & \gamma_i(\bar{k}_i, \omega) = \frac{1}{\rho_0 \omega^2} \left(\frac{e_{15}^0}{\eta_{11}^0} \right)^2 \frac{\beta_\perp^2}{\bar{k}^2 - \beta_\perp^2} m_i \quad (4) \end{aligned}$$

In which,

$$\begin{aligned} \alpha^2 &= \frac{\rho_0 \omega^2}{C_{11}^0}, \\ \alpha^2 &= \frac{\rho_0 \omega^2}{C_{66}^0}, \beta_\perp^2 = \frac{\rho_0 \omega^2}{C_{44}^0}, \\ C_{44}^0 &= C_{44}^0 + \frac{(e_{15}^0)^2}{\eta_{11}^0} \quad (5) \end{aligned}$$

Rewrite again Eq. (4) as

$$\begin{aligned} \hat{f}_H^\alpha(x) &= \frac{1}{\Gamma(1+\alpha)} \int_{-\infty}^{\infty} \frac{f(t)}{(t-x)^\alpha} (dt)^\alpha \\ &= \frac{1}{\Gamma(1+\alpha)} \int_{-\infty}^{\infty} f(t) g(x-t) (dt)^\alpha \\ &= f(x) * g(x), \end{aligned} \quad (6)$$

$$\partial_j (C_{ijkl} \partial_k u_l + e_{kij} \partial_k \varphi) - \rho \ddot{u}_i = 0 \quad (7)$$

$$\partial_j (e_{ijkl} \partial_k u_l - \eta_{kij} \partial_k \varphi) = 0 \quad (8)$$

The linear equation can be expressed into the following simplified forms:

$$\begin{aligned} L(\nabla, \omega) f(x, \omega) &= 0 \\ L(\nabla, \omega) &= T(\nabla) + \omega^2 \rho \mathbf{J} \quad (9) \end{aligned}$$

In which,

$$\begin{aligned} T(\nabla) &= \begin{Bmatrix} T_{ik}(\nabla) & t_i(\nabla) \\ t_k^T(\nabla) & -\tau(\nabla) \end{Bmatrix}, \mathbf{J} = \begin{Bmatrix} \delta_{ik} & 0 \\ 0 & 0 \end{Bmatrix}, \\ f(x, \omega) &= \begin{Bmatrix} u_k(x, \omega) \\ \varphi(x, \omega) \end{Bmatrix} \quad (10) \end{aligned}$$

The Proteus simulation circuit is shown as the Fig. (2). Open a microcontroller property window of the parts, add the above compiled target code files at "Program File" menu, and input the crystal frequency 11.0592MHz at "Clock Frequency" field. The simulation results are shown as the Fig. (3).

IV. EXPERIMENT RESULT

The whole design is realized through Verilog HDL 2001, and without FPGA IP cores, so the proposed design belongs to independent platform that can be applied to any FPGA module such as Xilinx and Actel. Nevertheless, Xilinx ISE9.2i is used in the FPGA implementation experiment in this paper, and simulation of performance function uses Questa Sim 10.0b which is matched with Xilinx Virtex-5 FPGA. Fig. 4 shows the implementation of hardware test system of the proposed design, including COMTECH modem for modulated input, Tektronix TLA5201B logic analyzer for capturing and observing the output of demodulator.

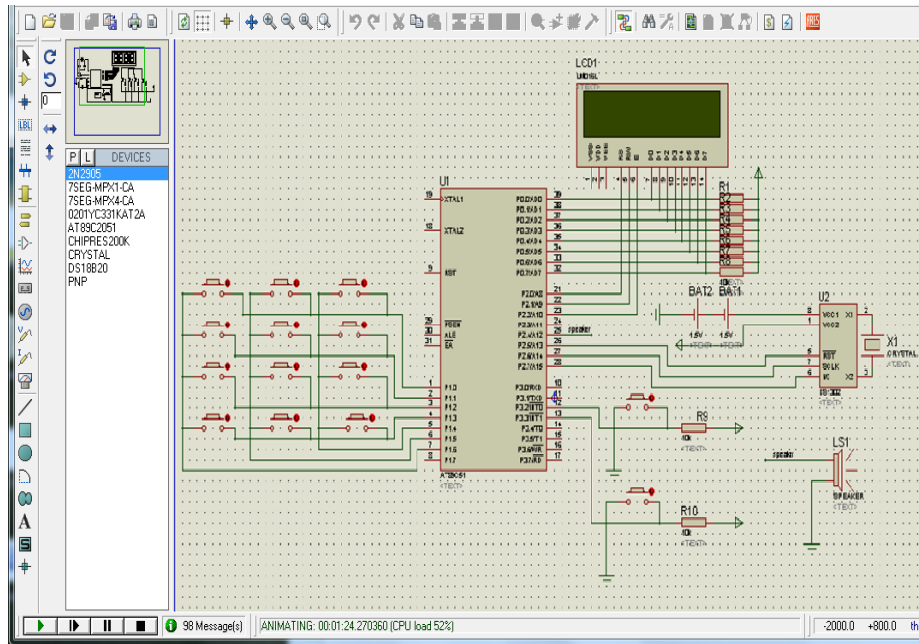


Figure 2. The simulation circuit diagram

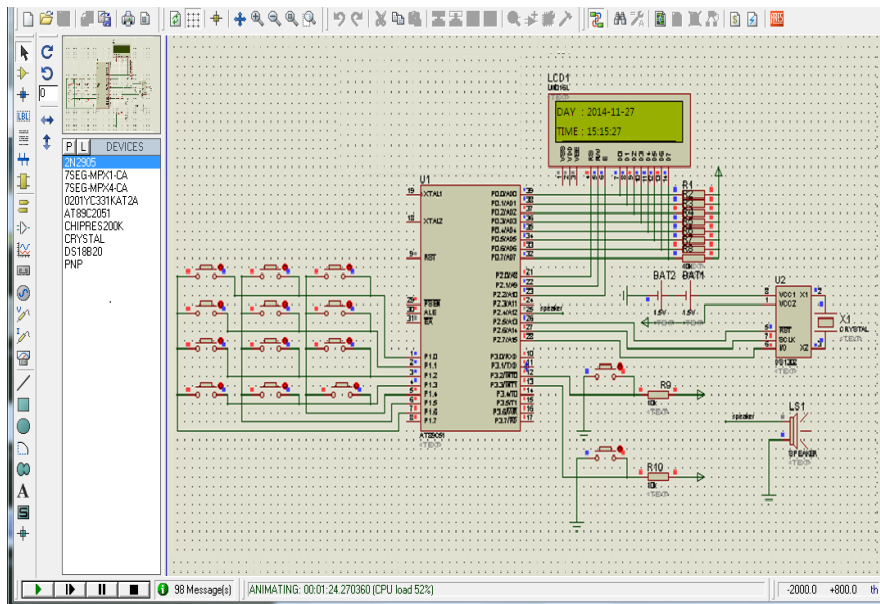


Figure 3. The circuit simulation diagram

Matlab is a high-level language with high efficiency used in scientific engineering calculation. It is also good at visual display of data in that it is capable of showing data's two, three or even four dimensional manifestations. Fig. 5 and Fig.6 show respectively the robot's working space drawn with Matlab's three dimensional plotting function plot3 and its projection on Plane xoz.

Since the differential equations have important applications in the natural sciences, technology and population dynamics, there is a permanent interest in obtaining sufficient conditions for the oscillation or non-oscillation of the solutions of various types of even-order/odd-order differential equations; see references in this article, and their references.

If x is a positive solution of (1), then the corresponding function $z(t) = x(t) + p(t)x(\tau(t))$ satisfies:

$$z(t) > 0, z^{(n-1)}(t) > 0 \quad (11)$$

$$z^{(n)}(t) < 0$$

Assume that $\alpha \geq 1, c, d \in \mathbb{R}$. If $c \geq 0, d \geq 0$, then

$$c^\alpha + d^\alpha \geq \frac{1}{2^{\alpha-1}}(c+d)^\alpha \quad (12)$$

By the definition of convex function, we have

$$f\left(\frac{c+d}{2}\right) \leq \frac{f(c)+f(d)}{2} \quad (13)$$

That is,

$$\frac{1}{2^{\alpha-1}}(c+d)^\alpha \leq c^\alpha + d^\alpha \quad (14)$$

So we get the equation (12). This completes the proof.

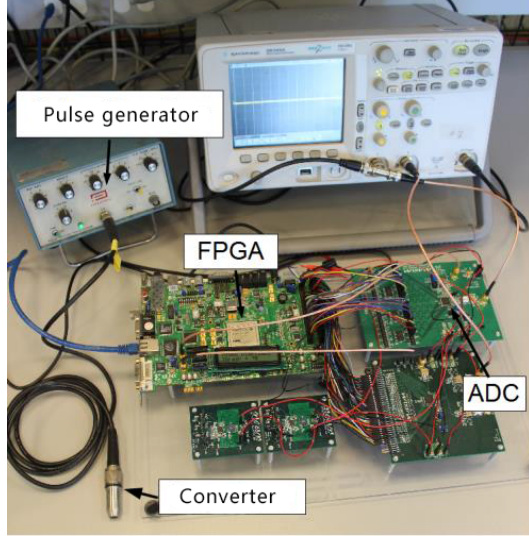


Figure 4. Diagram of Hardware test system

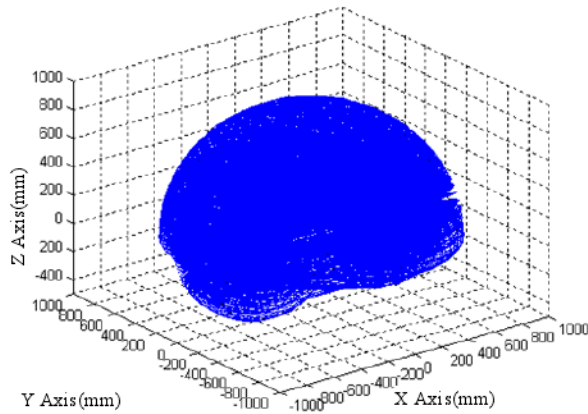


Figure 5. The working space for robot

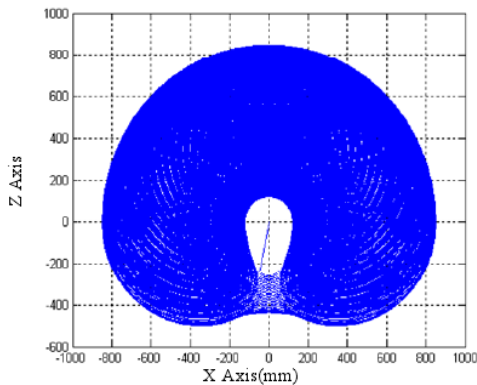


Figure 6. The Projection of the working space on Plane XoZ

Next, we establish our main results. For the sake of convenience, let

$$Q(t) = \min \{q(t), q(\tau(t))\} \quad (15)$$

Assume that

$$\int_{t_0}^{\infty} t^{n-1} Q(t) dt = \infty \quad (16)$$

Further, assume that the first-order neutral differential inequality

$$\begin{aligned} & \left(y(t) + \frac{P_0^\alpha}{b} y(\tau(t)) \right)' + \frac{Q(t)}{2^{\alpha-1}} \\ & \left(\frac{\lambda}{(n-1)!} \sigma^{n-1}(t) \right)^\alpha y^\alpha(\sigma(t)) \leq 0 \end{aligned} \quad (17)$$

V. DISCUSSION

Test of the forward kinematics solution. The forward kinematics solution for the 4 DOF robot is theoretically solved according to D-H transformation of the robot joint coordinate system. Experiments are done to test and verify the correctness of the forward kinematics solution and the robot performance. Six groups of the joint variables are chosen randomly from the robot joint space. The robot starts motion from zero point. The actual positions of the manipulator in the robot base coordinate frame are measured. The six groups of the joint variables are substituted into the forward kinematics solution equation to obtain the theoretical position. The test result of the forward kinematics solution can be obtained with actual position compared with the theoretical position.

Traditional grid map every vertex has 4 edge neighbors and 4 vertex neighbors. The traditional grid map provides four moving direction choices for each location. Triangular mesh map we can see that every triangle has 3 edge neighbors and 9 vertex neighbors, so it has 12 cell neighbors in a non-boundary triangle cell.

The triangle mesh map provides 12 moving direction choices for each location, and we know that the triangle one has good precision, high efficiency and facility of dealing with geo-character, such as rupture line, construction line which results in a much smoother path compared with the traditional grid map. This series of figures and table we show different path developed with different cost functions in different terrain models to see the influence of smoothing process basing in triangular B-spline method.

In the comparison principle in (7) we do not assume that the deviating arguments are either delay or advanced type, and hence this result is applicable to all types of equations. Further, the comparison principle established in (7) reduces oscillation of equation (1) to find conditions for the first-order neutral differential inequality (5) has no positive solution. Therefore, applying the conditions for equation (5) to have no positive solution, one can immediately get oscillation criteria for equation (1). The result of calculation shows that the robot's working space V equals 1.92m³, and the volume index reaches 0.64. The simulation results prove such designed robot meets the expectations for eggplant in greenhouse and is able to work more efficiently. The simulation validates the rationality of the structure design.

After analysis, the TD parameter is opposite and independent. So the controller parameters located between the

ESO and NLSEF. In order to coordinate influence between the two parameters, we use particle swarm optimization algorithm to optimize the main performance parameters. Base coordinate is selected in turret turning center. The robot moved on the z coordinate plane motion which digging. Scoop is equivalent to manipulators grippers at the end and target above can be used to identify shovel and bucket tilt can be used to identify bucket attitude.

VI. CONCLUSION

The robot obstacle avoidance and path planning in static scenes is the core content of the global path planning as well as the basis of the local path planning. In order to improve the real time performance, accuracy and stability, an obstacle avoidance strategy of mobile robot based on wireless sensor networks is proposed in this paper. Multiple mobile robots system provides an unchallenged incentive to all researchers in the past two decades, with its distribution characters in time and space, as well as its high efficiency. The algorithm is combined with fuzzy control and neural network control theory which can express those rules difficult to describe by using mathematical model. Great interests have been attracted to application domains including industry, military, national defense, daily life, and deep space, etc.

The key of obstacle avoidance planning is to formulate feasible strategy, so that, according to a certain standard, the robot can move from the start point to the target point without collision, so, a method is needed to solve the mobile robot obstacle avoidance planning problem based on the combination of clone selection algorithm and visual graph, in the course of the study, set the length of path as the standard of obstacle avoidance planning results, hunt for optimal path in a structured environment, then control the entity robot base on the optimal path. In the research of specific application tasks, such as transporting heavy object, arresting target and multi-sensors cooperative map exploration, etc., robots are required to form and maintain specific shapes of formation during the tasks' execution. The result of calculation shows that the robot's working space V equals 1.92m^3 , and the volume index reaches 0.64. The simulation results prove such designed robot meets the expectations for eggplant in greenhouse and is able to work more efficiently. The simulation validates the rationality of the structure design. So the simulation results show that the obstacle avoidance strategy can improve the overall system performance substantially and is suitable for mobile robot intelligent control.

REFERENCES

- [1] K. S. Chia, and X. Y. Yap, "A Portable PID Control Learning Tool by means of a Mobile Robot," *International Journal of Online Engineering*, vol. 12, no.6, pp. 54-57, June 2016. <https://doi.org/10.3991/ijoe.v12i06.5716>
- [2] H. Jing, "Node deployment algorithm based on perception model of wireless sensor network," *International Journal of Automation Technology*, vol.9, no.3, pp. 210-215, April 2015. <https://doi.org/10.20965/ijat.2015.p0210>
- [3] H. Jing, "Routing optimization algorithm based on nodes density and energy consumption of wireless sensor network," *Journal of Computational Information Systems*, vol. 11, no.14, pp. 5047-5054, July 2015.
- [4] X. Wei, K. Jia, J. Lan, et al., "Automatic method of The object extraction under complex agricultural background for vision system of The robot," *Optik - International Journal for Light and Electron Optics*, pp. 125-129, 2014.
- [5] N. Pereira, F. Ribeiro, G. Lopes, et al., "Jorge. Autonomous golf ball robot design and development," *The Industrial Robot*, pp. 396-402, 2012.
- [6] Z. Zhang, D. He, L. Jing, et al., "Picking robot arm trajectory planning method," *Sensors & Transducers*, vol. 162, no.1, pp. 1621-1626, 2014.
- [7] Z. Zhang, J. Tang, I. Huang, et al., "Research on kinematics for inhibition fluttering of picking robot arm," *Sensors & Transducers*, vol. 161, no.12, pp. 161-171, 2013.
- [8] L. Wang, et al., "Mechanics and energetics in tool manufacture and use: a synthetic approach," *Journal of the Royal Society Interface*, pp. 111-114, 2014. <https://doi.org/10.1098/rsif.2014.0827>
- [9] D. Zou, W. Zhang, W. Qiang et al., "Design and implementation of a trusted monitoring framework for cloud platforms," *Future generations computer systems: FGCS*, vol. 29, no.8, pp. 2092-2102, 2013. <https://doi.org/10.1016/j.future.2012.12.020>
- [10] F. Tao, Y. Cheng, L.D. Xu, et al., "CCIoT-CMfg: Cloud Computing and Internet of Things-Based Cloud Manufacturing Service System," *IEEE transactions on industrial informatics*, vol. 10, no.2, pp. 1435-1442, 2014. <https://doi.org/10.1109/TII.2014.2306383>
- [11] L. T. He, and C. Hu, "Impacts of interval measurement on studies of economic variability: Evidence from stock market variability forecasting," *The Journal of Risk Finance*, pp. 85-101, 2007. <https://doi.org/10.1108/15265940710834771>

AUTHOR

AN Peng is with the College of Electronics and Information Engineering, Ningbo University of Technology, Zhejiang, China (anp04@nbut.edu.cn).

The paper is supported by the National Natural Science Foundation of China under Grant (No.61502256) and Zhejiang Provincial Natural Science Foundation of China under Grant (No. LY15F020011). Submitted 09 September 2016. Published as resubmitted by the authors 19 November 2016.